ISSN: 2639-7455

Research Article

Earth & Environmental Science Research & Reviews

Analyzing A Planet That Crosses a Small Comet's Fragment Chain

Hamid A. Rafizadeh*

Emeritus Professor, Bluffton University, USA.

***Corresponding Author**
Hamid A. Rafizadeh, Emeritus Professor, Bluffton University
Adjunct Professor, University of Dayton, Present Address: 320 Northview Road, Oakwood, OH 45419, USA.

Submitted: 2024 Mar 04; **Accepted**: 2024 Apr 16; **Published**: 2024 Apr 22

Citation: Rafizadeh, H. A. (2024). Analyzing A Planet That Crosses a Small Comet's Fragment Chain. *Earth Envi Scie Res & Rev, 7*(2), 01-14.

Abstract

This study explores the novel concept of a planet intersecting the orbit of a small comet's fragment chain. Utilizing a simple multi-generational model of comet fragmentation, it analyzes the planet's interaction with the comet's fragment chain and simulates probability distributions for both chain crossing and fragment capture. This model offers insights complementary to impact theories that seek to explain the Younger Dryas boundary. Moreover, the potential presence of cometary material in Earth's orbit due to crossing a comet's fragment chain could profoundly influence climate patterns, with far-reaching implications for global agriculture and food production.

Keywords: Planetary Science; Comets; Comets Dynamics; Impact Processes; Planetary Dynamics

1. Introduction

The interaction between the solar system's small bodies and planets is a complex composite of collisional and non-collisional events. A significant area of focus in this realm involves studying the impact of small bodies on planets or their satellites, a perspective that has yielded notable success. For instance, it elucidates the abrupt extinction of dinosaurs resulting from an asteroid-Earth collision approximately 65 million years ago. Another compelling illustration is the more recent collision of fragments from the comet Shoemaker–Levy 9 with Jupiter, providing further validation of the collisional emphasis in the interactions between the solar system's planets, satellites, and cosmic bodies [1-4].

However, the understanding of these interactions goes beyond singular collisions, encompassing a spectrum of non-collisional events in planet-small body dynamics. This spectrum ranges from tidal disruptions to various cosmogenic factors influencing the evolution of a small body's orbit, eventually leading to the formation of a meteoroid stream [5]. In the evolutionary transition of a small body into a meteoroid stream, it is acknowledged that planets may traverse through these streams. Such passages can be characterized by meteoroids impacting the planets [6]. Additionally, considering the history of fragmentation of small bodies, it is crucial to recognize that the planet currently traversing the meteoroid stream might have, at some point, passed through the parent chain of the meteoroid stream, specifically the fragment chain comprised of large fragments.

Currently, a wealth of collisional evidence supports the formation of fragment chains. The impact cratering on a planetary scale serves as a tangible manifestation of the fragment chain's formation and its collisional history. On planets devoid of atmospheres, impact craters are well-preserved; however, on Earth, the observation of impact cratering is complicated by factors like weathering and burial [7]. These impacts are identified as rare and catastrophic interactions between the planet and a fragment chain [8]. The striking example of the Shoemaker-Levy 9 fragment chain, etching a series of crater-like dark spots on Jupiter's gaseous surface, further reinforces the perception of rare and catastrophic planet-fragment chain interactions.

For the possibility of a planet passing through a comet's fragment chain, the current exploration is primarily confined to meteoroid streams. In prevailing theories, meteoroid streams are compositions of extraterrestrial bodies offering insights into the formation and evolution of cosmic bodies [9, 10]. This perspective does not point out the potential for a planet to traverse an earlier iteration of the meteoroid stream, specifically the fragment chain

featuring large fragments. Even in the context of unraveling the evolutionary progression of meteor showers, meteoroid streams, and dormant comets, the objective is not to develop a comprehensive understanding of the fragment chain but rather to identify the parent comet [11-15]. For instance, employing a tidal breakup model, the information on chain length and fragment numbers is leveraged to only estimate the size of the parent comet [16-22].

2. Comet Fragmentation Models

Sekanina pioneered a two-parameter model for split comets, grounded on the concept of gradual fragment separation [23]. This model posits that the rate of separation is influenced by the differences in the solar attractions of the fragments. Initially developed to fit the observations of 13 split comets, Sekanina's model evolved into multiparameter versions, enhancing its applicability to 21 known split comets [24-26]. The versatility of Sekanina's multiparameter model is evident in its application to Shoemaker–Levy 9 (SL9) [27]. A numerical iteration, employing ephemeris-determination code and an iterative least-squares differential-correction optimization procedure, refines the model's fit to SL9 observations [28].

In the current exploration of fragment chain dynamics, the focus is directed towards specific interactions among fragments. Sekanina and Chodas introduced a numerical model illustrating that in the Kreutz system of sungrazing comets, the motion of one fragment can be deduced from the known motion of another fragment [29, 30]. Another model, utilizing a back-and-forth orbit integration technique, enhances the understanding of two subgroups within the Kreutz sungrazer system, positing that these subgroups originated from the progenitor's breakup into two superfragments [31]. A refinement of this two-superfragment model is found in the cascading fragmentation model [32]. Additional numerical models focus on the parent comet of the Kreutz family of sungrazers, exploring the scenarios of whether it was a Centaur, a comet injected from the Oort cloud, or a comet initially injected from the Oort cloud in a non-sungrazing orbit, later evolving into a sungrazing orbit [18].

In their examination of Jupiter family comets (JFC) and the population proportion undergoing splitting within a defined range of perihelion distance q, Di Sisto et al. develop a model for a comet's splitting frequency f expressed as $f = f_0(q/q_0)^{-\beta}$, where f_0 and q_0 and β are model parameters [33]. Numerical simulations were conducted using an assembled sample comprising 95 real and 905 fictitious comets. The model parameters were adjusted to align the orbital element distribution of the assembled sample with observational data. During simulations, a random number z between 0 and 1 was compared to the splitting frequency f. If $z < f$, a splitting event occurred; otherwise, no splitting event took place. This process generated 52 splitting models with varying β values (0, 0.5, 1, 1.5, and 2) and f_0 ranging from 0.1 to 2. Using a χ^2 test, the top four models were identified by comparing their fit to the orbital parameter distributions of the assembled sample. However, no different than other split comet models, Di Sisto et al.'s models are limited to the JFC population, constrained by the assembled sample.

Exploring the interactions between a planet and the fragment chains offers a promising avenue for investigating the Younger Dryas boundary. This event, occurring approximately 12,800 years before present (BP), marks a significant climate cooling episode associated with widespread biomass burning, megafauna extinction, and the decline of the Paleoindian Clovis culture [34, 35]. Evidence, such as platinum deposition, high-temperature spherules, meltglass, and nanodiamonds across multiple continents, suggests a global phenomenon [36]. Some propose that the cause was Earth encountering a fragment or fragment swarm from a 100-km-diameter comet from the Centaur system in an earth-crossing orbit [37, 38].

Building upon Di Sisto et al.'s model of comet fragmentation and chain formation [33], Napier hypothesizes that the Younger Dryas impact resulted from Earth encountering a comet's fragment chain [39]. Napier utilizes the top three models from Di Sisto et al.'s selection to develop fragment chains for a 100-km-diameter comet in an Encke-like orbit. The dominant process of comet disintegration in Napier's model is splitting, supported by the observation that cascading fragmentation is the primary mode of comet disintegration [40, 41]. Napier's calculations predict 750–1500 splitting events over timescales of 6000–20,000 years, suggesting that the resulting meteor intensities could contribute to the climatic conditions observed during the Younger Dryas event. However, these models share the limitations of both Di Sisto et al.'s models and the Encke-like orbit, restricting their generalizability.

Two crucial insights emerge from the fragmentation models developed for split comets such as SL9, the Kreutz family of sungrazers, and JFC population. Firstly, these models are invaluable tools precisely tailored to individual comets, utilizing narrow windows of observational data. The comet-specific models address fundamental questions surrounding why comets split, how to calculate the motion of one fragment based on another's known motion, and how to discern the progenitor of comet fragments. Secondly, while these models are highly useful for specific cases, they fall short of serving as a universal framework capable of providing a comet's "multi-generational fragment distribution." To explore the lifecycle study of a planet crossing a comet's fragment chain, a more encompassing model is imperative, one that provides general multi-generational fragment distributions. The conspicuous absence of such a universal multi-generational model within the current repertoire of comet fragmentation models underscores this article’s efforts to develop a general, multi-dimensional model of comet fragmentation and fragment separation. Establishing such a foundational framework is crucial for the subsequent exploration of a planet interacting with a comet's fragment chain.

3. Model Description

This article presents a simple multi-generational model of a comet's

fragment chain, aiming to analyze a planet's interaction with the fragment chain and its potential for capturing fragments. Illustrated in Fig. 1, the model specifically examines the planet's interaction with the parent chain rather than the meteoroid stream, with the fragment chain having a planet-intersecting orbit. The fragment chain's orbit, at the point of intersection, may not necessarily align with or be close to the ecliptic, despite the common occurrence of such alignments in the solar system.

As depicted in Fig. 1, when observing the solar system from above the north ecliptic pole, both planets and the majority of comets and their fragment chains exhibit a counterclockwise revolution around the Sun. The statistics related to 1720 known comets with elliptical orbits reveals that 1608 (93.5%) follow counterclockwise orbits with 930 being short period and 790 long period comets [42]. The article emphasizes the significance of a planet intersecting a comet's fragment chain with an elliptical counterclockwise orbit. This interest is attributed to the repetitive chain crossings facilitated by the elliptical orbit and the synergistic counterclockwise motion of both the planet and the fragment chain, contributing to an enhanced likelihood of fragment capture.

In the broader context, the various mechanisms responsible for the creation of a comet's fragment chain are delineated as catastrophic disruption, tidal forces, rotation, thermal stress, gas pressure, and impacts [40]. These mechanisms are found to be common among both active and dormant comet nuclei in the inner solar system, with resulting fragment chains having the potential to evolve into planet-crossing paths [43]. Notably, the Shoemaker-Levy 9 case stands out, where the tidal breakup mechanism is well understood [41, 44, 45].

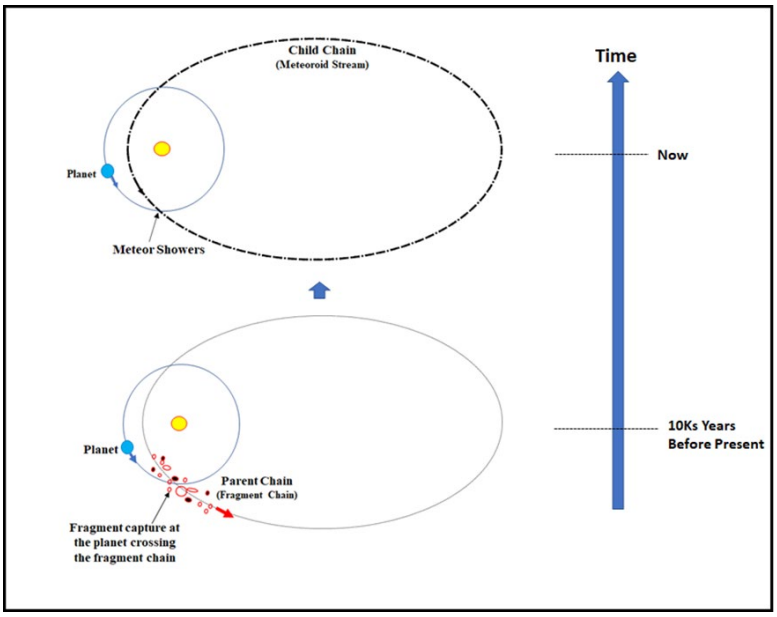

Fig. 1. A comparative perspective on the interaction between the planet and comet fragmentation. In an earlier generation, the planet engages in chain-crossing with the *parent chain* (a fragment chain), while in a later generation, the planet will only cross the *child chain* (the meteoroid stream).

It is well-established that, in the absence of an intervening mechanism or structural reconfiguration, a planet cannot alter the trajectory of a comet or its fragment chain, hindering the potential for capturing them in planet-centric orbits. At best, it produces a small population of temporarily captured orbiters (TCO) and minimoons, with the largest TCO in the steady state population being about 1–2 m in diameter [46, 47]. Consequently, capture theories must invoke dissipative mechanisms, such as tidal friction that disperses fragments and influences their motion. Additionally, a resisting medium, if sufficiently dense, can impact fragment motion, as can fragment collisions [48, 49].

Within the scope of modeling a planet crossing a comet's fragment chain, this article emphasizes the crucial role of relative velocities as the key dissipative mechanism contributing to fragment capture, when both the planet and the fragment chain move counterclockwise with linearized orbits at the point of intersection [50]. The low relative velocities increase the probabilities of successful fragment capture [51]. With a smaller intersection angle θ, the planet and the fragment chain nearly align in direction, with a relative velocity of $\bar{V}_p - \bar{V}_{fc}$, where $\bar{V}_p$ is the planet's velocity and $\bar{V}_{fc}$ is the fragment chain's velocity at the point of intersection. The small intersection angle θ and the reduced relative speed $|\bar{V}_p - \bar{V}_{fc}|$ serve as indicators of the strength of the dissipative mechanism, slowing down the planet relative to the fragment chain and facilitating successful fragment capture.

The introduction of the multi-generational model of the fragment chain lays the foundation for the subsequent analyses. That is followed by modeling and calculation of the probabilities

associated with the planet crossing the fragment chain and capturing fragments. Finally, concluding observations encapsulate the study's findings.

4. Method

Using a multi-generational Graphical Sequence Model (GSM), this study analyzes the formation of a comet's fragment chain and assesses the probability of a planet crossing the fragment chain and capturing fragments. The GSM framework assumes that a comet is comprised of an initial clump of fundamental units, and in each generation's fragmentation, each clump undergoes breakdown into nf smaller clumps, which then separate as a generational unit at ns separation units, each of the length ds. The parameters nf and ns define the pattern of fragmentation and fragment separation for the chain within each generation. This process is described and shown graphically in Figs. 2 and 3.

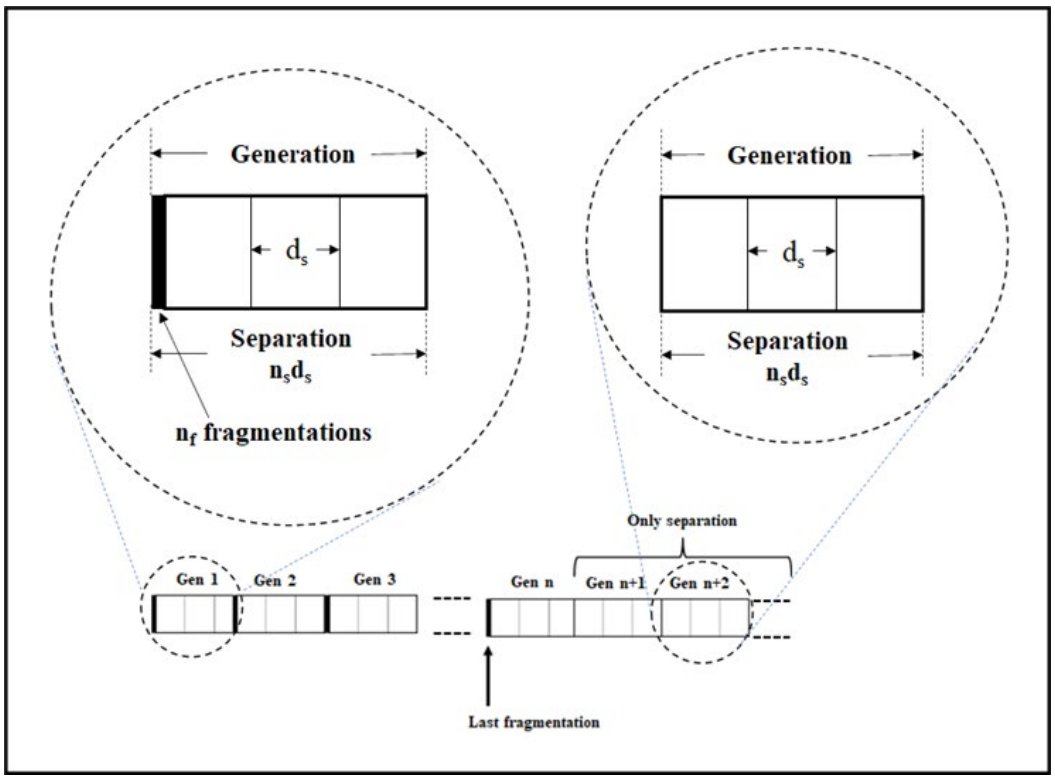

Fig. 2. The multi-generational Graphical Sequence Model (GSM) adopts a modular structure. Within each generation, the fragmentation into nf clumps is followed by the separation of clumps by ns separation units, each of the length ds. The fragmentation terminates when the comet breaks up into fundamental units, at which point the generational module exclusively involves fragment separation.

Within each generational module of the GSM, the individual clump will break into nf new clumps, which subsequently disperse and separate by $n_s d_s$, where d_s represents the separation unit. In the subsequent generation, each clump from the preceding generation replicates this modular pattern of fragmentation and separation. This sequence of generations persists until reaching the n_{max} generation, wherein the breakup of clumps from the previous generation into fundamental units is fully completed. Beyond this point, subsequent GSM generations are characterized solely by the separation module, devoid of any further fragmentation. Consequently, the fragment chain, comprised exclusively of fundamental units, progressively elongates as fragments from each generation separate and disperse by n_s units, each of the length d_s.

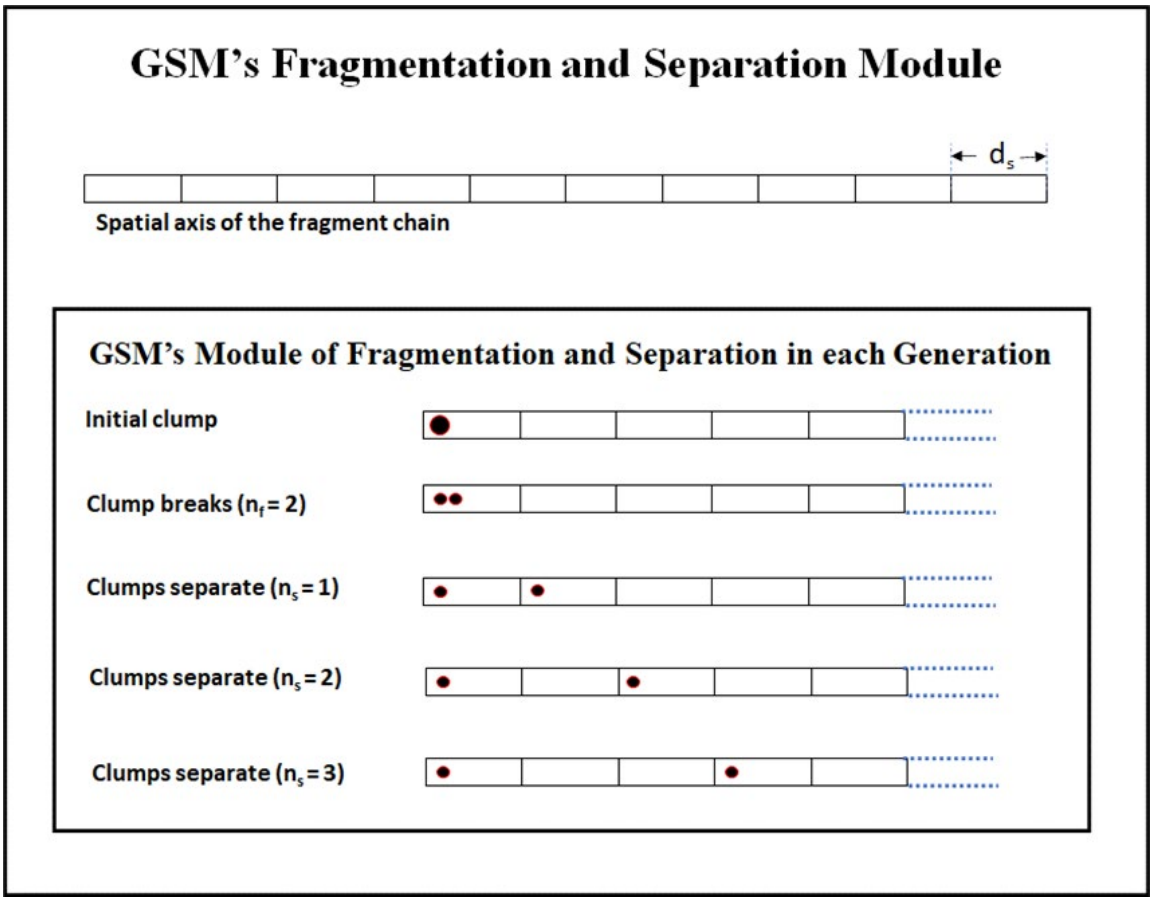

Fig. 3. Illustrating the Graphical Sequence Model (GSM) for a single generation with $n_f = 2$, wherein each clump in the initial generation undergoes division into two clumps. Noting that within a fragment chain, the sequence of generations would only use a single n_s value, to elucidate the concept, here three instances of clump separation are presented for $n_s = 1$, 2, and 3.

5. Fragment Chain's Length and Fundamental Fragment

In GSM, each set of n_f and n_s values creates a graphical sequence that can be expressed in the form of a generational recursive equation for L_n, the length of the comet's fragment chain. These equations are transformed into a general explicit equation for the length of the comet's fragment chain:

$$L_n = [n_f n_s - (n_s - 1) + n_s (n_f - 1) (n - 1)] d_s. \quad (1)$$

This equation provides the length of the comet's fragment chain for any given values of n_f and n_s within any generation n. It is noted that this general equation represents the first explicit formulation for the lifecycle length of a comet's fragment chain in terms of the fragmentation and separation parameters n_f, n_s, and n.

To apply Eq. (1) and determine the length of a comet's fragment chain, the GSM requires two essential pieces of information: the size of the parent comet and the total number of fragments within the comet. Calculating the total number of fragments necessitates defining a "fundamental unit" for fragments—the minimum fragment size. This fundamental unit represents the smallest fragment that avoids further fragmentation, preventing an endless chain of fragmentation. In GSM, the parent comet is envisioned as a cluster of fundamental units. During each generation's fragmentation stage, a cluster breaks down into nf smaller clusters, which then separate as a generational unit at ns separation units, each of the length d_s.

GSM's modular fragmentation and separation process leads to a maximum value of n, denoted as n_{max}, determined by the total number of fundamental fragments in the comet. At n_{max}, the comet has disintegrated into fundamental units that no longer undergo fragmentation. The fragment chain at n_{max} comprises N_o fundamental units that initially constituted the parent comet's clump. Beyond n_{max}, the fragments only undergo separation. Before reaching n_{max}, the length of the fragment chain is determined by the distance between its two farthest clumps. At n_{max} and beyond, the length of the fragment chain is dictated by the separation between the two farthest fundamental fragments within the chain.

Having conceptually defined the fundamental fragment, GSM calculations require a specific size for this fundamental unit. While various methods exist for estimating the fundamental fragment's size, such as catastrophic tidal disruption [52, 53], or fitting to SL9

fragments [54], they are inconsistent with this article's objective of developing a simple, multi-generational model for studying a planet crossing a comet's fragment chain. Therefore, in alignment with Asphaug and Benz, the fundamental fragment's size in GSM calculations is chosen as the typical 720-meter-diameter fragment of SL9 where the 2-km-diamter SL9 comet breaks down into 21 fundamental fragments [17]. In comparison, in the volumetric, SL9-normalized model, a 100-km-diameter comet would have N_o = 2.625 million fundamental fragments.

In general, the number of clumps in generation n, denoted as N(n), is given by

$N(n) = (n_f)^n$, or

$n = (\log_{10}N(n)/\log_{10}n_f)$

The maximum value of n, denoted as n_{max}, is determined by

$n_{max} = (\log_{10}N_o/\log_{10}n_f)$

where N_o represents the initial number of fundamental fragments in the comet. For a 100-km-diameter parent comet with nf.= 2, n_{max} will be 21.32 while for n_f= 6, n_{max} will drop to 8.25.

6. The Fragment Chain of a Specific Comet

In setting up the GSM calculations, various considerations come into play concerning the size of a small comet and its mode of fragmentation and fragment separation defined by the parameters n_f and n_s. Through exploration of different comet sizes and different values of n_f and n_s, the analytical conclusions and significant patterns are observed to remain the same for the planet crossing the fragment chain of a generation. As such, we only focus on a specific example in this section, where a small comet with a diameter of 3.14 km is considered. This comet is composed of a clump of 81 SL9-type fundamental fragments, with fragmentation and fragment separation defined by n_f = 3 and n_s = 2, setting nmax at 4. It is noteworthy that this comet could be classified as either a long-period or a short-period comet, and both possibilities are considered in the subsequent calculations.

Fig. 4 shows the fragment distributions of the first four generations of the comet's fragment chain. In the first generation, the parent comet breaks up into three clumps, each consisting of 27 SL9-type units. The three clumps are separated by n_s = 2 separation units, each ds in length. In the second generation, each of the three clumps from the first generation undergoes fragmentation and separation based on n_f = 3 and n_s = 2. This creates a fragment chain characterized by its peak at 27 fragments, made of three clumps, each consisting of nine SL9-type units. The continuation of modular fragmentation and fragment separation produces the distribution for generation 3 with a peak of 21, made up of seven 3-unit clumps. GSM characterizes the seven clumps as overlapping clumps (OCs) that do not aggregate to form a single 21-unit clump.

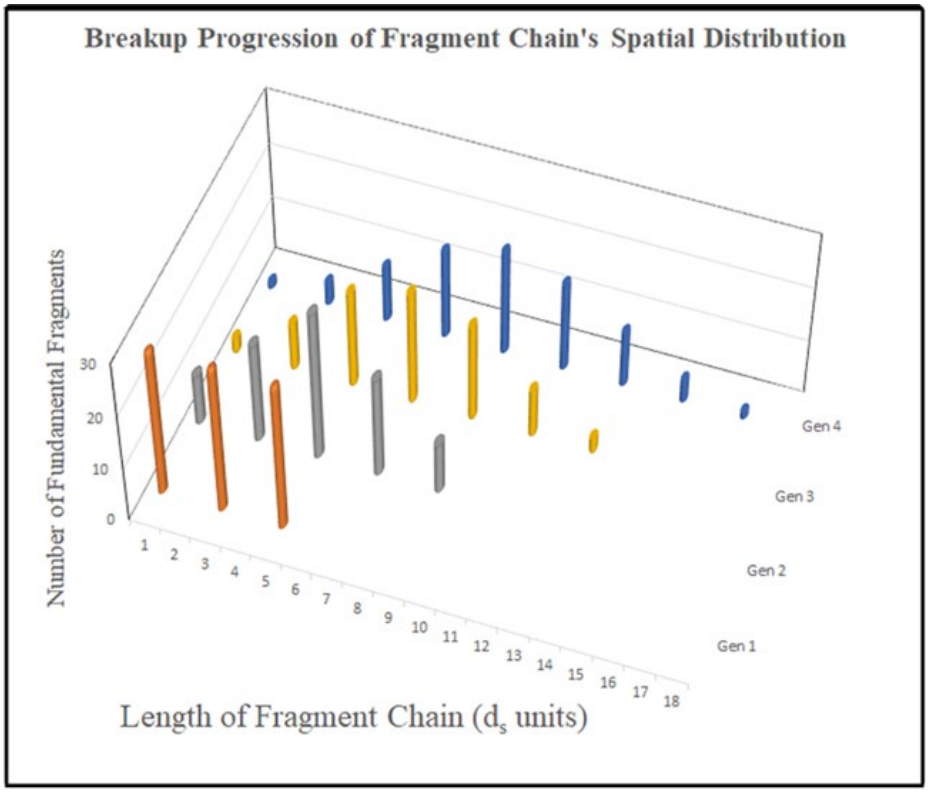

Fig. 4. The distribution of fragment in the fragment chain of a 3.14-km-diameter comet, consisting of 81 fundamental fragments with n_f = 3 and n_s = 2, may correspond to either a long period or a short period comet.

In generation 4, the fragmentation and fragment separation exhaust the entire reservoir of SL9-type fundamental fragments for the 3.14-km-diameter comet. In this stage, generation 4 exhibits a fragment distribution devoid of clumps, with its peak comprised of 19 fundamental fragments. According to GSM, these 19 fundamental fragments at the peak of the fragment chain are characterized as overlapping fundamental fragments (OFFs), distinct from clumps as they do not aggregate in this generation to form clumps. In GSM, clumps originate solely from the fragmentation of the parent comet before the fragment chain reaches the generation designated as n_{max}. After generation 4, the fragmentation process ceases, and fragments of each subsequent generation only undergo separation.

In simulation of generation 2, 44.39% of the instances of the planet crossing the fragment chain involve passage through empty space, resulting in no encounter with any fragments. This percentage increases to 46.8% in generation 4 and further to 47.49% in generation 6. Across generations, as the fragment chain lengthens, the number of fragments the planet encounters diminishes. The average number of fragments crossed in generation 2 is 8.98, decreasing to 4.81 in generation 4 and further to 3.32 in generation 6.

The next section explores the modeling and simulation of the probabilities associated with chain crossing and the likelihood of fragment capture during chain crossing.

7. Probability Calculations

The fragment chain can be conceptualized as an elongated cylinder with diameter *d*, intersected by the planet at an angle θ. In this configuration the planet crosses a long cylindrical chain, resulting in a transient period during which the planet effectively resides within the fragment chain. In this context, two crucial parameters come into focus: the length of the planet's trajectory within the chain and the duration of time the planet remains within the confines of the chain.

Assuming a cylindrical geometry for the fragment chain with diameter *d* and the intercept angle θ, the path traversed through the chain would have the length $l_p = d/\sin(\theta)$. The crossing time, t_c, is then calculated as $t_c = l_p / |\bar{V}_p - \bar{V}_{fc}|$, where $\bar{V}_p$ is the planet's orbital velocity, $\bar{V}_{fc}$ the fragment chain's velocity at the point of crossing, and $|\bar{V}_p - \bar{V}_{fc}|$ the relative speed. As a preliminary, order-of-magnitude calculation, assuming a relative speed of 10 km/s, Table 1 shows the time that the planet will take to cross the fragment chain. The crossing time is of the order of minutes to a few hours, presenting opportunities for the planet to capture fragments in orbit around it within this timeframe. In the following sections, the probabilities of chain crossing and fragment capture will be simulated and analyzed.

Chain-crossing time (hours)		Fragment Chain Diameter (10^3 km)		
		1	**5**	**10**
Intercept angle (°)	**5**	0.32	1.59	3.19
	10	0.16	0.80	1.60
	15	0.11	0.54	1.07

Table 1. The duration of the planet residing within the fragment chain while crossing it.

In the dynamic interplay between the planet and the fragment chain, two distinct probabilities come to the forefront: the likelihood of the planet crossing a fragment chain and the probability of capturing fragments as the planet traverses the fragment chain. The probability of the planet crossing a fragment chain is contingent upon several factors, including the length of the fragment chain, the orbital length of the fragment chain, and the relative velocity between the planet and the fragment chain at the point of intersection. In an extreme scenario where the fragment chain transforms into a meteoroid stream enveloping the entire orbit, the probability of crossing the chain becomes a certainty, given the intercepting orbits.

Using Eq. (1) to determine the length of the fragment chain, and defining Lo as the fragment chain's orbital length, the probability of the planet crossing the fragment chain can be formulated. Assuming intersecting orbits of the planet and the fragment chain, the probability per perihelion passage, Pcross, can be approximated by:

$$P_{cross} = L_n/L_o \quad (2)$$

Different methods exist for calculating L_o. It can be determined by calculating the circumference of the ellipse of the fragment chain's orbit using equations based on orbital parameters [55, 56]. This method necessitates the specification of the fragment chain's orbital parameters. Another method determines L_o from the fragment chain's average orbital speed v_o and orbital period P_{orb} as

$$L_o = v_o P_{orb}$$

Napier used this method to calculate P_{cross} in Earth crossing the fragment chain of an Encke-type comet [39]. In this article this method is refined and broadened, leveraging a more comprehensive approach that calculates the orbital length using the distributions of v_o and P_{orb} derived from the Minor Planet Center (MPC) database encompassing all known comets [42]. The distributions of orbital periods for elliptical orbits of 930 short period and 790 long period comets yield peak values of 10 years for short period comets and 300 years for long period comets. Similarly, short period comets

exhibit an average v_o of 12.24 km/s, and a peak of 15 km/s. In contrast, long period comets show an average v_o of 1.13 km/s, with peak a 0.4 km/s.

For both short period and long period comets, the peak regions in the distributions of both v_o (orbital velocity) and P_{orb} (orbital period) serve as parameters in the simulation calculations based on Eq. (2), the chain crossing probability. For short period comets, the peak area for v_o spans from 4 to 17 km/s, encompassing 99.03% of the comets in the distribution. Meanwhile, the peak area for P_{orb} ranges from 0 to 45 years, covering 88.6% of the comets in the distribution. In the case of long period comets, the peak area for v_o falls within the 0 to 3.6 km/s range, capturing 99.48% of the comets in the distribution. However, for P_{orb}, the peak area of long period comets is comparatively limited, extending from 200 to 1200 years and encompassing only 20% of the comets due to the distribution's long tail.

With the knowledge of these peak area distributions for v_o and P_{orb}, the orbital length is then calculated in kilometers. However, to determine L_n the length of the fragment chain in kilometers, it is essential to quantify the GSM's unit of separation, d_s. To develop an estimate of ds, the data from comet Shoemaker-Levy 9 (SL9) is used as a benchmark for inferring the general physical properties of comets [53]. The fragment chain of SL9, initially detected in April 1993, extended to approximately 5 million kilometers by July 1994 [45]. Designating this length as L_{SL9}, and inserting it into Eq. (1), an estimate for the ds can be derived as:

$$d_s = L_{SL9}/[n_f n_s - (n_s - 1) + n_s (n_f - 1) (n - 1)] \quad (3)$$

In determination of the fundamental separation length d_s from Eq. (3) and SL9 data is subject to four constraints. These constraints include the parent comet breaking into 21 fragments, the resulting fragment chain reaching a length of about 5 million km, the fragment chain having a "string of pearls" configuration, and the fragment chain forming within the first few generations of the parent comet breakup. Through an exploration of values of n, nf, and ns within GSM's modular structure, it was revealed that satisfying the "string of pearls" constraint was only feasible if the parent comet possessed a weak rubble-pile structure, breaking into 21 fundamental fragments in the first generation. Any value of n_f below 17 failed to create the string of pearls and maintain the 5 million km length. Similarly, the constraints pushed ns values toward 1 or 2. Based on these observations, the representative GSM-based values for SL9's fragment chain were determined as $n_s = 1$ and $n_f = 21$, leading to an estimated fundamental separation unit d_s of approximately 250,000 km. This value is used in subsequent simulation calculations.

A simulation program is used in calculating the chain crossing probability for the fragment chains of the 3.14-km-diameter comet [57]. Fig. 5 provides a comparative analysis of the probability of the planet crossing the generation 4 of the fragment chain from the 3.14-km-diameter comet, which can be either a short period or a long period comet. Notably, the peak probability for the short-period comet exceeds that of the long-period comet. The pattern observed for the two probability distributions in Fig. 5 is similar to those of generations 2 and 6, not shown. The 3.14-km-diameter comet, when classified as a short-period comet, yields higher probabilities for chain crossing compared to its classification as a long-period comet, primarily driven by the differences in the distributions of v_o and P_{orb} which influence the chain crossing probability calculation.

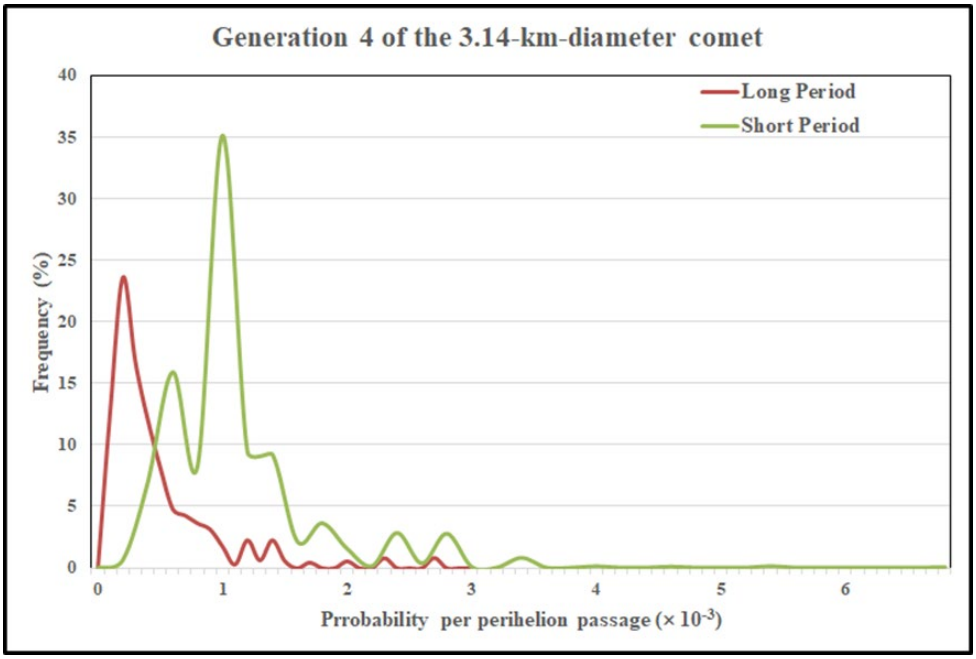

Fig. 5. The probability of the planet crossing the generation 4 of the fragment chain of a 3.14-km-diameter comet, which may be classified as either a short period or a long period comet.

The key observation is that, irrespective of the generational length of the fragment chain or the distributions of orbital velocity and orbital period influencing the comet's classification as either short period or long period, the probability of chain crossing—given the interception of the planet and the fragment chain orbits—remains on the order of 10^{-3} per perihelion passage. This probability is higher than the comet-planet collision probability, which for both short period and long-period comets, stands at approximately 10^{-9} per perihelion passage [58-60].

8. Probability of Fragment Capture

The concept of capture involves converting a fragment's orbit from chain-centric to planet-centric. In order to assess the probability of fragment capture during chain crossing, it is imperative to compute both the eccentricity *e* and the semi-minor axis *b*. The capture conditions include eccentricity *e* being less than one and the semi-minor axis *b* exceeding the planet's radius *R*. Meeting these criteria ensures that the captured fragment is in orbit around the planet rather than on a trajectory to escape or impact the planet. In the process of calculating $P_{capture}$, the eccentricity e is derived from the fragment velocity and position using the equation [61]:

$$\bar{e} = [(V^2 - \mu/r)\,\bar{r} - (\bar{r} \bullet \bar{V})\,\bar{V}]/\mu$$
$$e = |\,\bar{e}\,|$$

where $\bar{V}$ is the relative velocity of the planet and fragment, namely $\bar{V}_p - \bar{V}_{fc}$, $\bar{V}_p$ the planet velocity and $\bar{V}_{fc}$ the fragment chain velocity at the point of intersection. $\bar{r}$ is the XYZ position of the fragment, and μ the gravitational parameter which, for an earthlike planet, has the value 3.986×10^5 km^3 s^{-2}. Since the planet's orbit intersects the fragment chain's orbit at the angle θ, $\bar{V}_p$ is oriented at the angle θ relative to $\bar{V}_{fc}$.

In $P_{capture}$ calculation, the semi-minor axis *b* is determined from eccentricity and semi-major axis *a* as [61]:

$$b = a\sqrt{(1-e^2)}$$

where semi-major axis a is

$$a = -\tfrac{1}{2}\,\mu / (V^2/2 - \mu/r)$$

The comet's velocity is given by [64]:

$$|\bar{V}_{fc}| = \sqrt{[GM\,(2/r - 1/a)]}$$
$$r = a\,(1 - e^2)/(1 + e\cos f)$$

e is the eccentricity, a the semi-major axis of the cometary orbit, r the heliocentric distance of the comet, *f* the angle from periapsis—the true anomaly, and GM the heliocentric gravitational constant, 1.3271×10^{11} km^{3}s^{-2}.

For perihelion velocity—$f = 0^o$, the equation for r reduces to r = q, where q is the periapsis distance, given by $q = a\,(1 - e)$. As illustrated in Fig. 1, in the configuration for the planet crossing the comet's fragment chain, the relevant crossing velocities mostly lie in the *f* range from 0 to 90 degrees. At $f = 90^o$, the equation for r reduces to $r = q\,(1 + e)$.

Using the Minor Planet Center (MPC) database of the known comets, an average difference of 27% is observed in comet velocities at the f values of 0^o and 90^o. Consequently, the expected crossing velocities in Fig. 1 configuration would fall within 27% of the perihelion velocities. As such, perihelion velocities provide a reasonable approximation for crossing velocities. Given the distribution of perihelion velocities for all known long period and short period comets, between 20 to 40 km/s lie 59% of the perihelion velocities for long-period comets and 83% for short-period comets [42]. In light of this observation, when simulating the probability of fragment capture, the fragment chain speed $|\bar{V}_{fc}|$ is selected to vary within the range 20 to 40 km/s.

As illustrated in Figs. 2 and 3, within the framework of GSM, the position of every clump or fragment is randomly situated within a single d_s space. To simulate this, the one ds space is partitioned into 20 segments, and the clump/fragment position is randomly assigned to one of these segments within the d_s space. As the planet crosses the chain, the fragments assume positions within the d_s space based on the random assignments. The established velocity range for fragments is 20-40 km/s, and for the planet (assuming an Earth-like planet), the velocity is set at 30 km/s. In the simulations, the fragment chain aligns with the X axis at the point of the planet crossing the chain. During the crossing, all fragments move along the chain, linearized at the X axis where the fragment velocity is V_x with $V_y = V_z = 0$. The intersection of the planet and fragment velocities occurs at an angle θ, which is fixed at 5 degrees. The chain diameter is set at 5,000 km.

Given these parameters and defining capture as the transformation of a fragment's chain-centric orbit into a planet-centric orbit, the probability of fragment capture at chain crossing can be expressed as:

$$P_{capture} = N(e<1,\, b>R) / N_{cross}, \qquad (4)$$

where N_{cross} is the total number of fragments crossed and $N(e<1, b>R)$ signifies the subset of fragments that meet specific criteria. Specifically, this subset comprises fragments with eccentricity *e* less than one, required for having an elliptical orbit around the planet. Additionally, the semi-minor axis *b* of the fragment's orbit must be larger than R, the planet radius. The condition $b > R$ ensures that the captured fragment is orbiting the planet, thus captured, than impacting the planet.

A key observation from the simulation results is that the probabilities of fragment capture, with an average of 5.84×10^{-2} per perihelion passage, remain higher than the comet-planet collision probability which for both short period and long period comets is of the order of 10^{-9} per perihelion passage [58-60].

Figs. 6 and 7 compare the fragments crossed and captured in generations 2, 4 and 6 of the 3.14-km-diameter comet. In generation 2, in 44.39% of the crossings, no fragments are encountered, leading to zero captures as the planet traverses empty spaces between the fragments. Compared to the total simulated crossings, only 5.34% of the fragments are captured. The average number of fragments captured is 8.98, with the maximum capture at a single crossing

being 27 fragments. Similarly, in generation 4 of the 3.14-km-diameter comet's fragment chain, in 46.8% of the crossings, the planet passes through empty spaces between fragments, resulting in zero captures. Among the total simulated crossings, a mere 5.75% of fragments are captured. The average number of captured fragments decreases to 4.81, with the maximum capture count at a single crossing being 19 fragments, both lower than the values observed in generation 2.

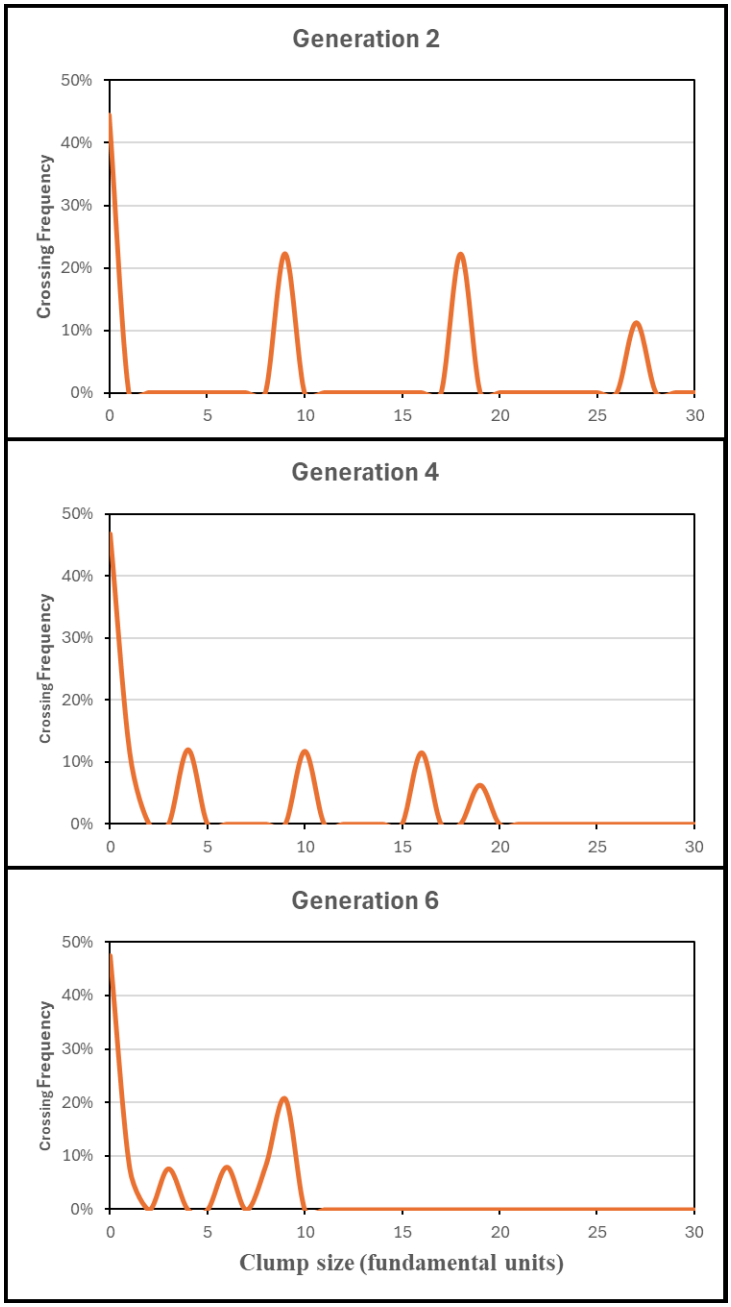

Fig. 6. The simulated fragments crossed the planet in generation 2, 4, and 6 of the fragment chain of the 3.14-km-diameter comet with $n_f = 3$ and $n_s = 2$.

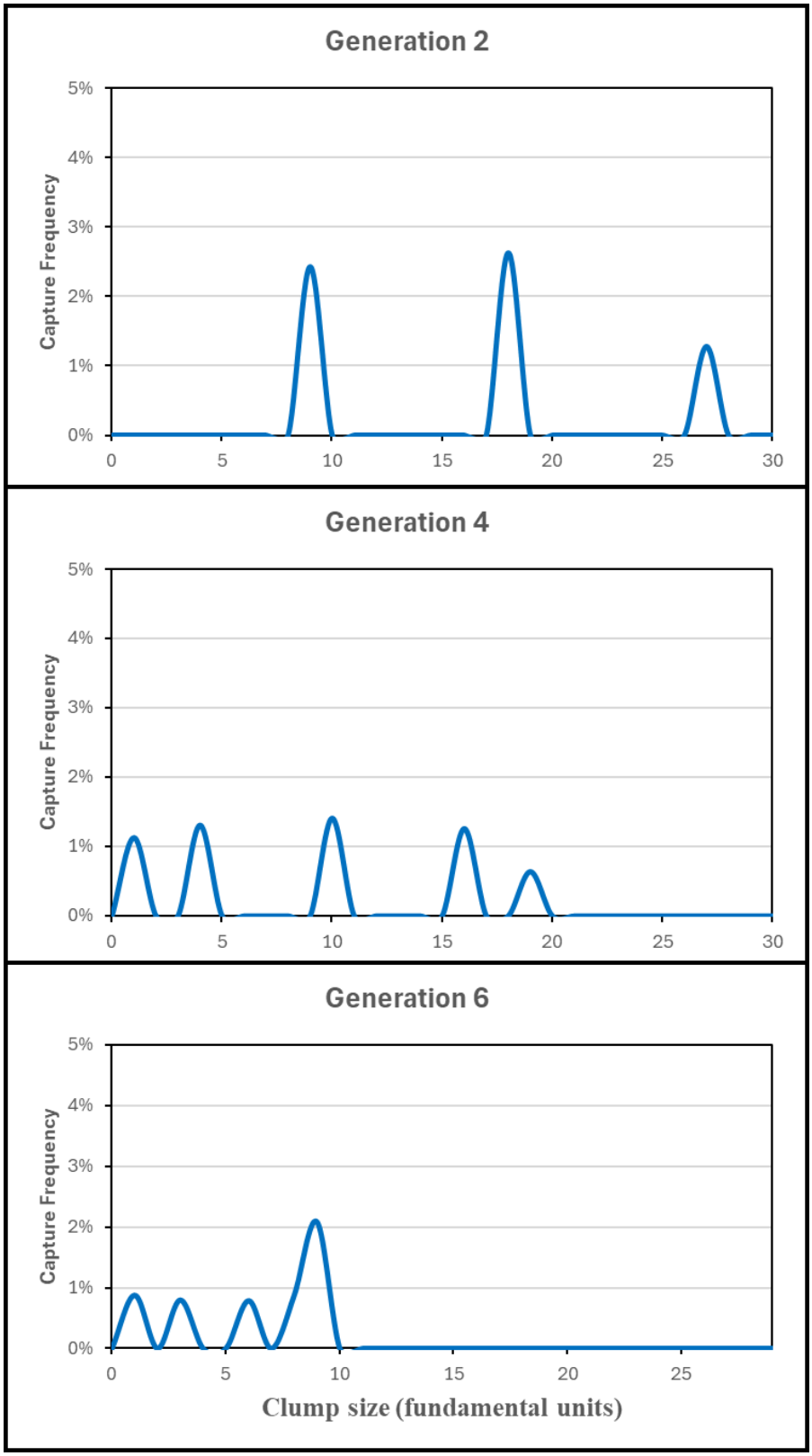

Fig. 7. The simulated fragments captured by the planet in generations 2, 4, and 6 of the fragment chain of the 3.14-km-diameter comet with $n_f = 3$ and $n_s = 2$.

When comparing the distribution of fragments crossed and captured, the size range of captured fragments in generation 6 is significantly constrained, encompassing only 9 fragments. In contrast, in generations 2 and 4, this range extended to 27 and 19 fragments, respectively. The visualization in Figures 6 and 7 indicates that in 47.49% of crossings in generation 6, no fragments are encountered, signifying the planet's passage through empty spaces between fragments. Of the total simulated crossings, only 5.44% of fragments are captured. The average number of captured fragments drops to 3.32, markedly lower than in generation 2, with the maximum captured at a single crossing reaching 9 fragments, also lower than the count observed in generation 2. This trend underscores the diminishing peak size and average size of the captured fragments across generations, reaching equilibrium in later generations. For the 3.14-km-diameter comet, the equilibrium peak of the fragment distribution is observed at 7 fragments beginning with the generation 7.

9. Conclusion

The novel idea of a simple, multi-generational Graphical Sequence Model (GSM) is formulated and applied to depict comet fragmentation and fragment separation within the context of a planet crossing a small comet's fragment chain. The GSM generates fragment distributions along the chain for each generation, facilitating calculations for the probability of the planet crossing the fragment chain per perihelion passage and the probability of fragment capture in chain crossing. For a 3.14-km-diameter long-period comet, the average probability of the planet crossing its fragment chain is 0.43×10^{-3} per perihelion passage, surpassing the planet-comet collision probability of 2.2×10^{-9} per perihelion passage for long-period comets [58, 59]. Similarly, for a 3.14-km-diameter short-period comet, the chain crossing probability is 1.01×10^{-3}, higher than the planet-comet collision probability of the order of 10^{-9} per perihelion passage for short-period comets [62, 63]. In both cases, the average probability of fragment capture in chain crossing is 5.84×10^{-2} per crossing. All calculated probabilities consistently point towards the planet crossing a fragment chain being a more probable event compared to the probability of a planet-comet collision.

The multi-generational GSM offers several advantages including the simplicity of developing a graphical representation of the fragment chain's distribution, ease of categorization of fragmentation and separation events using parameters nf, ns, ds, and n, and the conversion of the chain's graphic structure into a recursive equation. This equation is then transformed into an explicit equation for the length of the fragment chain with parameters nf, ns, and n, providing measures for the probability of the planet crossing the fragment chain and the probability of fragment capture in chain crossing. Finally, the GSM holds potential for refinement and improvement in future studies, especially in its application to phenomena like the Younger Dryas boundary. In this context, the model of a planet crossing a comet's fragment chain complements existing impact models. Such integration contributes to better understanding of Younger Dryas observations related to significant climate cooling, widespread biomass burning, megafauna extinction, and the decline of human population because of the adverse impact of climate on agricultural practices and food production.

Acknowledgement: I express my gratitude to Michael Rudenko of the Minor Planet Center for his invaluable assistance in analyzing the comet database.

References

1. Ipatov, S. I., & Mather, J. C. (2004). Comet and asteroid hazard to the terrestrial planets. *Advances in Space Research, 33*(9), 1524-1533.
2. Medvedev, Y. D., Bondarenko, Y. S., Vavilov, D. E., & Shor, V. A. (2016). Problems of asteroid–comet hazard. *Kinematics and Physics of Celestial Bodies, 32,* 223-226.
3. Shustov, B. M., Shugarov, A. S., Naroenkov, S. A., & Prokhorov, M. E. (2015). Astronomical aspects of cosmic threats: new problems and approaches to asteroid—comet hazard following the Chelyabinsk event of February 15, 2013. *Astronomy Reports, 59*, 983-996.
4. Sokolova, M. G., Nefedyev, Y. A., & Varaksina, N. Y. (2014). Asteroid and comet hazard: Identification problem of observed space objects with the parental bodies. *Advances in Space Research, 54*(11), 2415-2418.
5. Sokolova, M. G., Kondratyeva, E. D., & Nefedyev, Y. A. (2013). A comparative analysis of the D-criteria used to determine genetic links of small bodies. *Advances in Space Research, 52*(7), 1217-1220.
6. Neslušan, L., & Tomko, D. (2023). Long-period dynamical evolution of the meteoroid stream originating in comet 21P/Giacobini-Zinner. *Icarus, 392,* 115375.
7. Hietala, S., Moilanen, J., & Plado, J. (2022). Keurusselkä impact structure, Finland—Overview, new observations, and renewed interpretation of the size. *Meteoritics & Planetary Science, 57*(11), 2063-2080.
8. French, B. M., & Koeberl, C. (2010). The convincing identification of terrestrial meteorite impact structures: What works, what doesn't, and why. *Earth-Science Reviews, 98*(1-2), 123-170.
9. Bsdok, B., Altenberger, U., Concha-Perdomo, A. E., Wilke, F. D. H., & Gil-Rodríguez, J. G. (2020). The Santa Rosa de Viterbo meteorite, Colombia. New work on it's petrological, geochemical and economical characterization. *Journal of South American Earth Sciences, 104,* 102779.
10. Lipschutz, M. E., and Schultz, L. (2014). Meteorites. In: Spohn, T., Breuer, D., and Johnson, T. V. (Eds.), Encyclopedia of the Solar System. Amsterdam: Elsevier, 625–655.
11. Boehnhardt, H. (2003). Comet splitting—Observations and model scenarios. In *Cometary Science after Hale-Bopp: Volume 1 Proceedings of IAU Colloquium 186 21–25 January 2002, Tenerife, Spain* (pp. 91-115). Springer Netherlands.
12. Jenniskens, P. (2008). Mostly dormant comets and their disintegration into meteoroid streams: A review. *Advances in Meteoroid and Meteor Science,* 505-520.

13. Marsden, B. G., & Sekanina, Z. (1971). Comets and nongravitational forces. IV. *Astronomical Journal, 76*, 1135-1151.
14. Watanabe, J. I., & Sato, M. (2008). Activities of parent comets and related meteor showers. *Advances in Meteoroid and Meteor Science, 102,* 111-116.
15. Ye, Q. Z. (2018). Meteor showers from active asteroids and dormant comets in near-Earth space: A review. *Planetary and Space Science, 164*, 7-12.
16. Asphaug, E., & Benz, W. (1994). Density of comet Shoemaker–Levy 9 deduced by modelling breakup of the parent'rubble pile'. *Nature, 370*(6485), 120-124.
17. Asphaug, E., & Benz, W. (1996). Size, density, and structure of Comet Shoemaker–Levy 9 inferred from the physics of tidal breakup. *Icarus, 121*(2), 225-248.
18. Fernández, J. A., Lemos, P., & Gallardo, T. (2021). On the origin of the Kreutz family of sungrazing comets. *Monthly Notices of the Royal Astronomical Society, 508*(1), 789-802.
19. Harrington, J., de Pater, I., Brecht, S. H., Deming, D., Meadows, V., Zahnle, K., & Nicholson, P. D. (2004). Lessons from Shoemaker-Levy 9 about Jupiter and planetary impacts. Jupiter. *The Planet, Satellites and Magnetosphere, 1*, 159-184.
20. Scotti, J. V., & Melosh, H. J. (1993). Estimate of the size of comet Shoemaker-Levy 9 from a tidal breakup model. *Nature, 365*(6448), 733-735.
21. Solem, J. C. (1994). Density and size of Comet Shoemaker–Levy 9 deduced from a tidal breakup model. *Nature, 370*(6488), 349-351.
22. Solem, J. C. (1995). Cometary breakup calculations based on a gravitationally-bound agglomeration model: the density and size of Shoemaker-Levy 9. *Astronomy and Astrophysics, v. 302, p. 596, 302,* 596.
23. Sekanina, Z. (1977). Relative motions of fragments of the split comets.: I. A new approach. *Icarus, 30*(3), 574-594.
24. Sekanina, Z. (1978). Relative motions of fragments of the split comets: II. Separation velocities and differential decelerations for extensively observed comets. *Icarus, 33*(1), 173-185.
25. Sekanina, Z. (1979). Relative motions of fragments of the split comets: III. A test of splitting and comets with suspected multiple nuclei. *Icarus, 38*(2), 300-316.
26. Sekanina, Z. (1982). The problem of split comets in review. In *Comets* (pp. 251-287). Univ. of Arizona Press Tucson.
27. Sekanina, Z. (1997). The problem of split comets revisited. *Astronomy and Astrophysics, v. 318, p. L5-L8, 318*, L5-L8
28. Sekanina, Z., Chodas, P. W., & Yeomans, D. K. (1998). Secondary fragmentation of comet Shoemaker-Levy 9 and the ramifications for the progenitor's breakup in July 1992. *Planetary and space science, 46*(1), 21-45.
29. Sekanina, Z., & Chodas, P. W. (2002). Common origin of two major sungrazing comets. *The Astrophysical Journal, 581*(1), 760-769
30. Sekanina, Z., & Chodas, P. W. (2002). Fragmentation origin of major sungrazing comets C/1970 K1, C/1880 C1, and C/1843 D1. *The Astrophysical Journal, 581*(2), 1389-1398.
31. Sekanina, Z., & Chodas, P. W. (2004). Fragmentation hierarchy of bright sungrazing comets and the birth and orbital evolution of the Kreutz system. I. Two-superfragment model. *The Astrophysical Journal, 607*(1), 620-639.
32. Sekanina, Z., & Chodas, P. W. (2007). Fragmentation hierarchy of bright sungrazing comets and the birth and orbital evolution of the Kreutz system. II. The case for cascading fragmentation. *The Astrophysical Journal, 663*(1), 657-676.
33. Di Sisto, R. P., Fernández, J. A., & Brunini, A. (2009). On the population, physical decay and orbital distribution of Jupiter family comets: Numerical simulations. *Icarus, 203*(1), 140-154.
34. Moore, C. R., West, A., LeCompte, M. A., Brooks, M. J., Daniel Jr, I. R., Goodyear, A. C., ... & Bunch, T. E. (2017). Widespread platinum anomaly documented at the Younger Dryas onset in North American sedimentary sequences. *Scientific reports, 7*(1), 44031.
35. Wolbach, W. S., Ballard, J. P., Mayewski, P. A., Adedeji, V., Bunch, T. E., Firestone, R. B., ... & Kennett, J. P. (2018). Extraordinary biomass-burning episode and impact winter triggered by the Younger Dryas cosmic impact 12,800 years ago. 1. Ice cores and glaciers. *The Journal of Geology, 126*(2), 165-184.
36. Pino, M., Abarzúa, A. M., Astorga, G., Martel-Cea, A., Cossio-Montecinos, N., Navarro, R. X., ... & Kennett, J. P. (2019). Sedimentary record from Patagonia, southern Chile supports cosmic-impact triggering of biomass burning, climate change, and megafaunal extinctions at 12.8 ka. *Scientific reports, 9*(1), 4413.
37. Clube, S. V. M., & Napier, W. M. (1984). The microstructure of terrestrial catastrophism. *Monthly Notices of the Royal Astronomical Society, 211*(4), 953-968.
38. Steel, D. I., & Asher, D. J. (1996). The orbital dispersion of the macroscopic Taurid objects. *Monthly Notices of the Royal Astronomical Society, 280*(3), 806-822.
39. Napier, W. M. (2019). The hazard from fragmenting comets. *Monthly Notices of the Royal Astronomical Society, 488*(2), 1822-1827.
40. Boehnhardt, H. (2004). Split comets. *Comets II,* 301-316.
41. Fernández, Y. R. (2009). That's the way the comet crumbles: Splitting Jupiter-family comets. *Planetary and Space Science, 57*(10), 1218-1227.
42. Minor Planet Center (MPC). (2023). Orbital elements for all of the currently known comets. https://minorplanetcenter.net/iau/MPCORB/AllCometEls.txt.
43. Jenniskens, P. (2006). Broken comets. In: *Meteor Showers and their Parent Comets.* Cambridge: Cambridge University press, 377–396.
44. Kleyna, J. T., Ye, Q.-Z., Hui, M.-T., Meech, K. J., Wainscoat, R., Micheli, M., Keane, J. V., Weaver, H. A., and Weryk, R. (2016). The Progressive Fragmentation Of 332P/Ikeya-Murakami. *Astrophysical Journal Letters 827*, L26.
45. Sekanina, Z., Chodas, P. W., & Yeomans, D. K. (1994). Tidal disruption and the appearance of periodic comet Shoemaker-Levy 9. *Astronomy and Astrophysics (ISSN 0004-6361), vol. 289, no. 2, p. 607-636, 289,* 607-636.

46. Bolin, B., Jedicke, R., Granvik, M., Brown, P., Howell, E., Nolan, M. C., ... & Wainscoat, R. (2014). Detecting Earth's temporarily-captured natural satellites—Minimoons. *Icarus, 241,* 280-297.
47. Granvik, M., Vaubaillon, J., & Jedicke, R. (2012). The population of natural Earth satellites. *Icarus, 218*(1), 262-277.
48. Byl, J., & Ovenden, M. W. (1975). On the satellite capture problem. *Monthly Notices of the Royal Astronomical Society, 173*(3), 579-584.
49. Jewitt, D., & Sheppard, S. (2005). Irregular satellites in the context of planet formation. *Space Science Reviews 116*, 441-455.
50. JeongAhn, Y., & Malhotra, R. (2017). Simplified derivation of the collision probability of two objects in independent Keplerian orbits. *The Astronomical Journal, 153*(5), 235.
51. Wetherill, G. W., & Stewart, G. R. (1993). Formation of planetary embryos: Effects of fragmentation, low relative velocity, and independent variation of eccentricity and inclination. *Icarus, 106*(1), 190-209.
52. Hahn, J. M., & Rettig, T. W. (1998). Tidal disruption of strengthless rubble piles—a dimensional analysis. *Planetary and space science, 46*(11-12), 1677-1682.
53. Movshovitz, N., Asphaug, E., & Korycansky, D. (2012). Numerical modeling of the disruption of Comet D/1993 F2 Shoemaker–Levy 9 representing the progenitor by a gravitationally bound assemblage of randomly shaped polyhedra. *The Astrophysical Journal, 759*(2), 93.
54. Hahn, J. M., & Rettig, T. W. (2000). Comet Shoemaker–Levy 9 dust size and velocity distributions. *Icarus, 146*(2), 501-513.
55. Tian, J. F., & Yang, Z. H. (2023). Absolute monotonicity of the accuracy of Ramanujan approximations for perimeter of an ellipse. *Revista de la Real Academia de Ciencias Exactas, Físicas y Naturales. Serie A. Matemáticas, 117*(3), 135.
56. Villarino, M. B. (2008). Ramanujan's Perimeter of an Ellipse. *https://arxiv.org/pdf/math/0506384.pdf.*
57. Nester, D. (2019). Excel Simulation Package. Bluffton, OH: Bluffton University. https://homepages.bluffton.edu/~nesterd/MGT515/index.html.
58. Steel, D. I. (1993). Collisions in the Solar system–V. Terrestrial impact probabilities for parabolic comets. *Monthly Notices of the Royal Astronomical Society, 264*(4), 813-817.
59. Weissman, P. R. (1982). Terrestrial impact rates for long and short-period comets. In: Silver, L. T., and Schultz, P. H. (Eds.), Geological Implications of Impacts of Large Asteroids and Comets on the Earth, Geological Society of America—Special Paper 190. Boulder, CO: Geological Society of America, 15–24.
60. Zimbelman, J. R. (1984). Planetary impact probabilities for long-period comets. *Icarus, 57*(1), 48-54.
61. Hicks, K. D. (2009). *Introduction to astrodynamic reentry* AFIT/EN/TR-09-03 Air Force Institute of Technology.
62. Olsson-Steel, D. (1987). Collisions in the Solar System–IV. Cometary impacts upon the planets. *Monthly Notices of the Royal Astronomical Society, 227*(2), 501-524.
63. Weissman, P. R. (2007). The cometary impactor flux at the Earth. In: Valsecchi, G. B., Vokrouhlický, D., and Milani A. (Eds.), Near Earth Objects, our Celestial Neighbors: Opportunity and Risk, vol. 236 of IAU Symposium. Cambridge: Cambridge University Press, 441–450.
64. Hughes, D. W., & Williams, I. P. (2000). The velocity distributions of periodic comets and stream meteoroids. *Monthly Notices of the Royal Astronomical Society, 315*(3), 629-634.